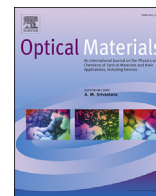




Contents lists available at ScienceDirect

Optical Materials

journal homepage: www.elsevier.com/locate/optmatOptimal performance of NdAl₃(BO₃)₄ nanocrystals random lasersAndré L. Moura ^{a,*}, Lauro J.Q. Maia ^b, Anderson S.L. Gomes ^c, Cid B. de Araújo ^c^a Grupo de Física da Matéria Condensada, Núcleo de Ciências Exatas – NCEX, Campus Arapiraca, Universidade Federal de Alagoas, 57309-005, Arapiraca, AL, Brazil^b Grupo Física de Materiais, Instituto de Física, Universidade Federal de Goiás, 74001-970, Goiânia, GO, Brazil^c Departamento de Física, Universidade Federal de Pernambuco, 50670-901, Recife, PE, Brazil

ARTICLE INFO

Article history:

Received 26 September 2016

Received in revised form

9 November 2016

Accepted 10 November 2016

Available online xxx

Keywords:

Random laser

Laser materials

Quantum defect

Thermal load

ABSTRACT

Resonant pumping associated with the influence of the quantum-defect between the excitation and the emitted laser photons allow optimal performance of neodymium ions (Nd³⁺) based random lasers (RLs), as demonstrated here for the first time. The RL emission at 1063.5 nm due to the Nd³⁺ transition ⁴F_{3/2} → ⁴I_{11/2} in a powder consisting of NdAl₃(BO₃)₄ nanocrystals, was investigated by exciting the powder at 690 nm, 750 nm, 810 nm, and 884 nm in resonance with the Nd³⁺ transitions from the ground state (⁴I_{9/2}) to the ⁴F_{9/2}, {⁴F_{7/2}, ⁴S_{3/2}}, {⁴F_{5/2}, ⁴H_{9/2}}, and ⁴F_{3/2} states, respectively. Although the Nd³⁺ absorption cross-section at 884 nm is smaller than those centered at 810 and 750 nm, excitation at 884 nm, that is in resonance with the emitting level, provided the smaller excitation pulse energy threshold and the larger slope efficiency due to the lower quantum defect.

© 2016 Elsevier B.V. All rights reserved.

1. Introduction

Laser emission in disordered systems [1,2], known nowadays as Random Lasers (RLs) [3], has attracted great attention from the fundamental and applied point of view after its first unambiguous demonstration in 1994 [4]. RLs are promising systems for several applications already proposed [5–8]. Among the most studied systems for RLs, those composed of glassy or crystalline powders doped with neodymium ions, Nd³⁺ [9,10], liquid solutions of dye and scatterers particles [11–14], semiconductor nanostructures [15–18], microstructured [19] and conventional [20,21] optical fibers, are highlighted. The Nd³⁺ based RLs are interesting because they are not photodegradable, have relatively high efficiency, and can lase in a wide range of wavelengths. RL emission around 1.06 μm has been observed in Nd³⁺ doped microparticles powders due to the electronic transition ⁴F_{3/2} → ⁴I_{11/2} [9,22–24]. In the reported studies, the population of the Nd³⁺ state ⁴F_{3/2}, the upper level of the laser transition, was achieved by exciting the powder at 532 nm and ≈808 nm, in resonance with the Nd³⁺ transitions ⁴I_{9/2} → {⁴G_{7/2}, ²G_{9/2}} [25,26], and ⁴I_{9/2} → {⁴F_{5/2}, ⁴H_{9/2}} [27], respectively.

Enhancement of Nd³⁺ based RLs performance is currently of great interest, and can be achieved by the identification of efficient

new host materials [9,28,29]. In another approach, the dependence of the RL performance due to the possible resonance with the Nd³⁺ transitions has been investigated by changing the excitation wavelength [23,27]. In this context, the quantum-defect (QD), defined as the difference between the energy of the excitation photons and the energy of the generated laser photons is known to affect the laser performance of conventional lasers [30–33], but was not discussed in the RLs literature. The QD energy is converted to thermal load by phonons that contribute for increasing the temperature of the host medium and for decreasing the laser performance by reducing the population difference between the upper and lower laser levels as well as by altering the Nd³⁺ stimulated emission cross section [34]. Then, as smaller the QD, larger can be the laser efficiency. In the case of Nd³⁺ doped materials, the influence of the QD associated with the 1.06 μm laser transition can be evaluated by exciting the medium with appropriate wavelengths in different Nd³⁺ absorption bands, as described below. In the optimum case reported here the wavelength excitation is in resonance with the emitting level, and this association led to an enhanced RL efficiency.

In recent works, the RL emission from powders of NdAl₃(BO₃)₄ particles, labeled as NdAB [22,24,27], was studied with respect to the dependence of the excitation pulse energy threshold, (EPE)_{th}, and slope efficiency with the excitation beam area [22], excitation wavelength [27], and also time behavior [24]. Previously the influence of the excitation beam wavelength (λ_{exc}) was studied by

* Corresponding author.

E-mail address: andre.moura@fis.ufal.br (A.L. Moura).

tuning λ_{exc} around the absorption band corresponding to the Nd^{3+} transition $4I9/2 \rightarrow \{^4F_{5/2}, ^4H_{9/2}\}$ [27] and the results were in good agreement with eqs. (1) and (2), presented in Ref. [23]:

$$\text{slope} = \eta(\lambda_{exc}) \frac{\lambda_{exc}}{\lambda_{em}}; \quad (1)$$

$$\frac{(EPE)_{th}}{A} \propto \frac{1}{\lambda_{exc} \eta(\lambda_{exc})} \sqrt{\sigma_{abs}(\lambda_{exc})}. \quad (2)$$

In eq. (1), $\eta(\lambda_{exc})$ is the powder absorbance at λ_{exc} , and λ_{em} is the RL wavelength. Eq. (2) shows an expression for the $(EPE)_{th}$ dependence with λ_{exc} , derived using the diffusion model applied to RLs. A is the focal area of the excitation laser and $\sigma_{abs}(\lambda_{exc})$ is the absorption cross-section at λ_{exc} . We emphasize that the λ_{exc} was tuned around a unique absorption band of the Nd^{3+} , and the influence of the QD on the performance of the NdAB RL was not fully investigated.

In the present paper, the QD influence on the performance of the RL based on the NdAB powder is reported; the choice of this material was motivated by its low $(EPE)_{th}$ for different excitation wavelengths.

2. Experimental details

The NdAB nanocrystals were synthesized by the polymeric precursor method using aluminum nitrate nonahydrate [$Al(NO_3)_3 \cdot 9H_2O$], neodymium hexahydrate [$Nd(NO_3)_3 \cdot 6H_2O$], boric acid (H_3BO_3), citric acid ($C_5O_7H_8$) as a complexing agent, and d-sorbitol ($C_6O_6H_{14}$) as polymerizing agent. The nanocrystals synthesis was achieved by dissolving aluminum and neodymium nitrates in an aqueous solution of citric acid at room temperature. Then, this solution was added to another solution of d-sorbitol and boric acid dissolved previously in water. The obtained solution was annealed at 150 °C in an oven to produce the polymerization process and to form a dried resin. The molar ratio of citric acid to elements (metals plus boron) was 3:1. The citric acid/d-sorbitol mass ratio was set to 3:2. The dried resin was calcinated at 400 °C during 24 h, heat-treated at 700 °C in the course of 24 h and finally annealed at 1150 °C during 5 min under rich-oxygen atmosphere. The particles' sizes, determined by electronic transmission microscopy, were in the range from 10 to 1000 nm with maximum at 55 nm.

Diffuse reflectance spectra were obtained by using a commercial spectrophotometer from 490 to 950 nm and $BaSO_4$ powder as reference.

Optical experiments were conducted as in Refs. [35,36]. The powder was placed in a sample-holder and gently pressed into a uniform disc region. The excitation source was an Optical Parametric Oscillator (OPO), tunable from 680 nm to 2200 nm, pumped by the second-harmonic of a Q-switched Nd:YAG laser (7 ns, 10 Hz). The output beam from the OPO was focused on the sample by a 10 cm focal length lens and the illuminated area was 1.2 mm², determined using a charged-coupled-device (CCD) camera having 1280 × 1024 squared pixels of size 5.2 μm. No significant variation of the illuminated area with the excitation wavelength was detected. The EPE was determined using a beam splitter and a calibrated photodetector coupled to an oscilloscope. The incident laser intensity on the sample was controlled by a pair of polarizers. The angle between the normal to the sample and the incident beam was 35° and the scattered light was collected from the front surface of the sample by a 5 cm focal length lens having diameter of 5 cm. The collected light was focused by a 20 cm lens at the entrance of a spectrometer (resolution: 0.024 nm) equipped with a cooled CCD. Optical filters were used to reject the excitation laser residue from the collected signal. The measurements were performed at room

temperature, around 22 °C. Eventual misalignment of the collected beam was ruled out by optimizing the alignment of the collected signal in the spectrometer for each excitation wavelength.

3. Results and discussion

In order to obtain laser emission at 1.06 μm, due to the transition $^4F_{3/2} \rightarrow ^4I_{11/2}$, the Nd^{3+} can be excited to states with energy larger than the $^4F_{3/2}$ state and on resonance with the $^4F_{3/2}$ state. In particular, at the wavelengths around 532 nm, 590 nm, 690 nm, 750 nm, 810 nm, and 884 nm, in resonance with the transitions starting from the ground state $^4I_{9/2}$ to the $\{^4G_{7/2}, ^2G_{9/2}\}$, $^2G_{7/2}$, $^4F_{9/2}$, $\{^4F_{7/2}, ^4S_{3/2}\}$, $\{^4F_{5/2}, ^4H_{9/2}\}$, and $^4F_{3/2}$ states, respectively, laser emission can be readily investigated. The transitions corresponding to the λ_{exc} used in the present work together with the laser transition at 1.06 μm are represented in Fig. 1.

To improve the RL performance, we first note that the QD could be minimized by exciting the Nd^{3+} at 884 nm in resonance with the transition $^4I_{9/2} \rightarrow ^4F_{3/2}$. However, this is not the most efficient excitation wavelength, since the RL efficiency depends also on $\eta(\lambda_{exc})$, among other parameters. The diffuse reflectance spectrum of the NdAB powder is presented in Fig. 2(a), from where one can conclude that the transitions at 588 nm, 750 nm and 810 nm have large $\eta(\lambda_{exc})$ with values that are about twice that corresponding to the transition at 884 nm. Probably, for this reason, most of the Nd^{3+} -based RLs reported in the literature were excited at ≈ 808 nm but, as shown below, this is not necessarily the best choice.

To determine which wavelength is the most appropriate for excitation of the NdAB RL, the powder was excited at 690 nm, 750 nm, 810 nm and 884 nm within the same EPE range. These wavelengths were chosen based on the spectrum of Fig. 2 (a) in order to maximize the fluorescence of the Nd^{3+} around 1.06 μm. The RL emission corresponding to each of these wavelengths was characterized by recording the fluorescence spectrum and monitoring the temporal decay of the $^4F_{3/2} \rightarrow ^4I_{11/2}$ transition at 1.06 μm for different EPE, as in Refs. [35,36]. Spectral narrowing is seen in Fig. 2 (b), which shows the spectra of the $^4F_{3/2} \rightarrow ^4I_{11/2}$ transition under excitation at 884 nm for EPE smaller (0.22 mJ) and larger (0.33 mJ) than the RL threshold of 0.30 mJ represented by the blue and red curves, respectively. Fig. 2 (c) shows the RL intensity dependence with the EPE for each excitation wavelength. In all cases, an abrupt growth in the slope of the curves is observed as the EPE exceeds a certain value corresponding to the RL threshold, $(EPE)_{th}$. The $(EPE)_{th}$ value was corroborated by the time behavior of the $^4F_{3/2} \rightarrow ^4I_{11/2}$ transition, as in previous works [35,36]. For $EPE < (EPE)_{th}$ a decay time of ≈ 10 μs was observed while for $EPE > (EPE)_{th}$ a signal with duration of ≈ 10 ns was recorded but limited by the resolution of the detection system.

The $(EPE)_{th}$ and the RL slope efficiency are plotted in Fig. 2 (d) as

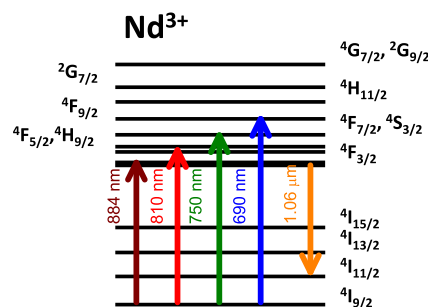


Fig. 1. Energy level diagram of the Nd^{3+} . The upward arrows represent transitions corresponding to the excitation wavelengths used in this work, and the downward arrow indicates the random laser transition.

Download English Version:

<https://daneshyari.com/en/article/5443084>

Download Persian Version:

<https://daneshyari.com/article/5443084>

[Daneshyari.com](https://daneshyari.com)